HOPKINS, DANIEL CORY. Characterizing the Spatial Variation in Particle Aggregation due to Heterogeneous Turbulence in a Flocculation Reactor. (Under the direction of Dr. Joel J. Ducoste)

ABSTRACT

A study was performed to investigate the impact of turbulent heterogeneity on aggregation and breakup in a flocculation reactor. The influence of the average characteristic velocity gradient (G), particle concentration, and coagulation mechanism on the flocculation performance was also investigated. Experiments were performed in a bench-scale reactor with a low-shear axial-flow impeller using a photometric dispersion analyzer (PDA) to examine the state of aggregation. Results indicated that floc growth increased while the floc size and variance in the floc size distribution decreased as G increased. In addition, floc growth, size, and floc size variance increased when the particle concentration of the water was increased and when moving from a charge neutralization mechanism to a sweep floc mechanism. Lastly, floc growth, size, and variance were found to vary spatially at low G values in the reactor with floc size and growth larger in the bulk region and the variance larger in the impeller discharge region.

CHARACTERIZING THE SPATIAL VARIATION IN PARTICLE AGGREGATION DUE TO HETEROGENEOUS TURBULENCE IN A FLOCCULATION REACTOR

by
DANIEL CORY HOPKINS

A thesis submitted to the Graduate Faculty of
North Carolina State University
in partial fulfillment of the
requirements for the Degree of
Master of Science

CIVIL ENGINEERING

Raleigh

2002

APPROVED BY:

_____
Dr. Allen Chao

_____
Dr. Francis de los Reyes

_____
Dr. Joel Ducoste
Chair of Advisory Committee

BIOGRAPHY

I was born on March (A), 1977 in (B). My family moved to (C), NC in the later part of (D) because my father obtained a new job with (E). The next (F) years of my life were spent here. I grew up addicted to sports thanks to my (G). When it was time to leave the nest, I chose to attend (H) and enrolled in the (I) program. After two and a half years and (J) additional course hours later, I finally settled down on a major in Environmental Engineering. I graduated with my bachelor's degree in 2000, but had not yet finished by my life in the world of (K). Therefore, I jumped right in to graduate school at North Carolina State even though I was also accepted to (L). The past two years of my life have been spent toiling over my course work and research with an emphasis in (M). I would fill you in on the rest of my future plans, but, hey, I don't even know. Anyway, to complete the story of my life, please answer the questions below. Enjoy!

A $\sqrt{121}$
B 3 words: not east but; the underside of your hand; rhymes with peach
C unscramble: I H L R G A E
D the year the Yankees won the World Series in baseball and Seattle Slew won the Triple Crown in horse racing
E This Company later merged with Memorex and begins with the letter T
F Age when you can become president minus 17
G Fill in the blank from this famous Star Wars quote: Luke, I am your ___!
H The school responsible for beating the 2002 NCAA National Champions (Maryland) in basketball in the semifinal of the ACC tournament that same year
I Fill in the blanks: F _ R _ _ _ E A _ C _ L _ E _ E
J A baker's dozen + 1
K unscramble: E C A A I M A D
L Played Florida State for the NCAA National Title in football in January, 2000
M The designation given for keeping the most abundant fluid in the world clean

ACKNOWLEDGEMENTS

The author would like to thank Nathan Jean and Jennifer King for their assistance in collecting useful data for analysis. Additionally, we would like to recognize Nathan Walsh for his assistance in experimental setup formulation and data collection.

TABLE OF CONTENTS

LIST OF FIGURES

LIST OF TABLES

INTRODUCTION

Flocculation is simply the process of generating particle interaction through turbulent mixing to form larger flocs that would successfully be removed in downstream solid/liquid separation processes (Letterman *et al.*, 1999). Turbulent mixing in a flocculation reactor is typically described by the average characteristic velocity gradient, G [s^{-1}] (Saffman and Turner, 1956):

$$G = \sqrt{\frac{\bar{\varepsilon}}{\nu}} \tag{1}$$

where $\bar{\varepsilon}$ is the reactor average turbulent energy dissipation rate and ν is the kinematic viscosity of the fluid. Currently, G is being used as a design parameter to determine the orthokinetic flocculation rate in reactors.

However, researchers have shown that G has shortcomings when describing the turbulent mixing in flocculators. Local energy dissipation rates were found to vary greatly between the impeller discharge region and the bulk region of the reactor (Schwartzberg and Treybal, 1968; McConnachie, 199; Ducoste *et al.*, 1997). In addition, some of the energy provided to the suspension in the reactor dissipates as heat at the impeller or at the walls of the reactor (Letterman *et al.*, 1999). Using G as described by Equation 1 in this sense assumes a homogeneous ε everywhere in the reactor that may be unrealistic when dealing with turbulent mixing involving impellers.

Extensive work has led to relating G with the steady-state maximum floc size of a suspension (Thomas, 1964; Parker *et al.*, 1972; Francois, 1987; Sonntag and Russel, 1987; Kusters, 1991). The steady-state maximum floc size is related to G as:

$$d_{max} = \frac{C}{G^n} \tag{2}$$

where d_{max} is the maximum steady-state floc diameter, C is the coefficient related to the binding energy of the floc particles, and n is the coefficient corresponding to the fractal dimension (D) of the floc, the floc breakup mode, and the size of the dissipative eddies in the fluid (Ducoste and Clark, 1998a). However, researchers have shown that the floc size distribution decreased with increasing reactor size regardless of impeller type at a constant G (Oldshue and Mady, 1978; Clark and Fiessinger, 1991; Clark *et al.*, 1994; Ducoste and Clark, 1998a). Additionally, changes in flocculation performance were also found when using different impeller types at constant G (Drobny, 1963; Argaman and Kaufman, 1970; Patwardhan and Mirajgaonkar, 1970; Hanson and Cleasby, 1990; Clark *et al.*, 1994; Sajjad and Cleasby, 1995; Ducoste and Clark, 1998a). In their study, Ducoste and Clark (1998a) attributed the change in the volume mean floc size to the turbulence intensity in the impeller discharge region and not to G. Therefore, considering that energy dissipation rate varies depending on reactor location, Ducoste and Clark (1998a) found that using G to calculate the d_{max} could be erroneous in floc size determination particularly in different reactor sizes, reactor geometries, or impeller types.

Numerical modeling conducted by Kramer and Clark (2000) furthered showed that using G, as determined by Camp and Stein (1943), covers up the influence of areas of high strain rates in orthokinetic coagulation. According to Kramer and Clark (2000), using G would signify that a homogeneous strain rate existed in the reactor. Yet, the strain rate is considerably greater in the impeller discharge region of the

reactor. Not incorporating strain rate and G fluctuations found within a reactor erroneously determined orthokinetic coagulation performance (Kramer and Clark, 2000).

In a recent study, Ducoste (2002) proposed that spatial variations in floc size distribution could exist at low G values making it possible for large flocs formed in the bulk region to be fractured primarily in the impeller discharge zone. Ducoste (2002) suggested that these large flocs could be broken up by larger scales of turbulent motion in the impeller discharge zone that cannot be described by the local energy dissipation rate. Further, it was proposed that the structure of these flocs would be different than those formed in the impeller discharge region and may be formed under different aggregation kinetics (Ducoste, 2002).

Spatial differences in the growth, size, and structure of flocs could be explained through a comparison of circulation and aggregation time scales. The circulation time in a reactor impacts the frequency of the exposure of flocs to the breakup in the impeller discharge region and is determined as follows:

$$\tau_c = \frac{V}{Q_p} \tag{3}$$

where V is the reactor volume and Q_p is the primary flow through the impeller discharge region boundary (Hsu and Glasgow, 1983). Typically, this time is multiplied by a factor between 6 and 10 to compensate for particles that may not follow the designated flow pattern created by the impeller of the reactor (Oldshue, 1983), thus requiring a greater amount of time to circulate through the impeller discharge region.

Aggregation time is determined as the elapsed time taken to develop flocs that are just visible. For orthokinetic aggregation of monodisperse fractal particles, the aggregation time can be computed as:

$$\tau_c = \frac{\pi D}{4\dot{\gamma}(3-D)}\phi_o^{-1}(1-q^{D-3}) \tag{4}$$

where $\dot{\gamma}$ is the shear rate/velocity gradient, ϕ_o is the volume fraction of primary particles, D is the fractal dimension of the particles, and q is the ratio of the size of the just visible floc to the primary particle size (Bremer *et al.*, 1995). D describes the space-filling ability and porous structure of a floc whose value ranges from 1 (a linear floc) to 3 (a compact, or space filling floc) (Selomulya *et al.*, 2001). Note that this equation is only valid for particles with $D < 3$. Kaolin clay particles, used in this study, have been shown to have flocs with $D \approx 1.8$ (Jiang and Logan, 1996). If the circulation time scales were much smaller than the aggregation time scales, then the local particle size distribution would not display any spatial variation in the reactor. If, however, the circulation time scales are on the same order of magnitude or larger than the aggregation time scales, then spatial variations in the floc size distribution could exist and possibly produce the scenario where larger flocs from the bulk region are fractured by large scale turbulent motion in the impeller discharge region (Ducoste, 2002).

In Equation 4, increasing the local volume fraction of particles and/or the shear rate can reduce the aggregation time scales. Researchers have shown that not only does the local shear rate vary spatially in the tank (Ducoste *et al.*, 1997), but there also may be zones where particles have been preferentially concentrated. Preferential

concentration is a phenomenon where dense particles accumulate around the periphery of vortices in fluid flow due to particle centrifugation from the vortex cores (Maxey, 1987; Squires and Eaton, 1991; Wang and Maxey, 1993; Eaton and Fessler, 1994). Studies have shown that the collision frequency rate may increase by as much as two orders of magnitude in regions where preferential concentration was found (Reade and Collins, 2000). The particle Stokes number (*St*), according to Reade and Collins (2000), appears to be the crucial parameter controlling preferential concentration. *St* is calculated as:

$$St = \frac{1}{18}\left(\frac{\rho_p}{\rho}\right)\left(\frac{\sigma}{\eta}\right)^2 \tag{5}$$

where ρ_p is the particle density, ρ is the fluid density, σ is the particle diameter, and η is the Kolmogorov length scale (Reade and Collins, 2000). Reade and Collins (2000) also explain that this phenomenon tends to occur at $St \approx 1$. For larger *St* values, shorter aggregation time scales can still occur as a result of particles dissociating with the fluid causing velocities between the particles to increase and, thus, trigger more frequent collisions (Reade and Collins, 2000).

Other researchers have shown that cluster-cluster aggregation tends to be favored on the boundaries between chaotic and non-chaotic flows (Danielson *et al.*, 1991; Hansen and Ottino, 1996). The result of cluster-cluster aggregation along these chaotic/non-chaotic boundaries is similar to that of preferential concentration in that cluster-cluster aggregation may also increase collision rates in the bulk region by at least one order of magnitude (Reade and Collins, 2000). Ducoste (2002) assumed that several non-chaotic flow regions might exist among the more prevalent chaotic flow

regions at low G values in the bulk region of the flocculation reactor. These chaotic/non-chaotic zones in the bulk region would foster cluster-cluster aggregation and assist in the production of larger flocs that can be fractured by large scales of motion in the impeller discharge region. Ducoste (2002) used this concept to explain conditions where tank size and impeller type can influence flocculation results under constant G. Escalating the collision rates in the bulk region as a result of cluster-cluster aggregation or preferential concentration indicates that aggregation time scales could be on the same order or less than circulation time scales at low G values. At higher G values, non-chaotic regions of flow may be less evident in the reactor. Yet, researchers have not investigated whether there are distinct differences in floc growth, steady-state size, and variance about the steady-state size in different reactor regions. This type of data would be necessary to confirm or refute the existence of spatial variation in floc growth, size, and variance and possibly explain some of the research studies involving scaleup/impeller type impact on flocculation performance.

The purpose of this study was to understand the impact of heterogeneous turbulence on flocculation performance, and, in particular, determine if there is spatial heterogeneity in the floc growth, average steady-state size, and variance. Using a photometric dispersion analyzer (PDA) the flocculation in a bench-scale flocculation reactor was examined. Floc growth, average steady-state floc size, and steady-state variance in floc size were determined at two reactor locations: the impeller discharge region and the bulk region. The influence of G (40 to 90 s^{-1}), synthetic raw water (SRW) particle concentration (50 or 100 mg/L), and coagulation mechanism (sweep floc or charge neutralization) on the flocculation performance was also investigated.

MATERIALS AND METHODS

SRW and coagulant solution

Three different experimental SRWs were developed in the study and are displayed in Table 1. The SRW tested in the flocculation experiments was made by mixing kaolin clay with deionized (DI) water. Average clay particle size was less than 1 μm in diameter. DI water was produced using a reverse osmosis/filtering system. 1 L kaolin clay slurries were developed to transfer the particles to the flocculation reactor. pH adjustment at the beginning of the flocculation experiment was achieved with the addition of H_2SO_4 or NaOH. Na_2CO_3 provided the desired alkalinity of the SRW. The chemical additions in Table 2 were determined after scaling up volumetric amounts computed using a titration technique (Greenberg *et al.*, 1992) from smaller volume samples.

Aluminum Sulfate ($Al_2SO_4 \cdot nH_2O$ where n is approximately 12-14) was the coagulant used in the flocculation experiments. Different volumetric amounts of a 1 g/L stock solution, comprised of alum and DI water, provided the coagulant concentration to be added to the SRW at the beginning of the rapid mix stage of the flocculation test. The amount of alum stock solution added at the beginning of rapid mix to provide sweep floc conditions was determined from jar test experiments. Sweep floc conditions are characterized by large amorphous floc formation at a pH = 8 (Reynolds and Richards, 1996). The final alum concentrate was determined from the jar test that produced the lowest settled water turbidity using the lowest alum concentration. The amount of the alum solution to add to provide charge neutralization conditions was also determined through jar tests and analyzed with Hemtrac's Model

ECA 2000P Electrokinetic Charge Analyzer. Charge neutralization conditions are characterized by a neutral charge in the water at a pH = 6. The final alum concentration was chosen from tests that produced an overall electrokinetic charge of zero. Table 3 provides the volumetric additions of the alum stock solution for each set of experimental conditions.

Experimental system

Figure 1 displays a schematic of the flocculation setup. The flocculation reactor was constructed out of 0.5 inch thick Plexiglas and has dimensions of 1.0ft L × 1.0ft W × 1.5 ft H. A metal support, harnessing the flocculation mixer, was centered and attached to two opposing sides of the reactor.

A Cole-Parmer Glas-Col Variable Speed Reversible Precision Stirrer provided the mixing for the flocculation step of the experiments. Attached to the stirrer shaft was an axial impeller with a diameter of 4.5 inches. The rapid mixer (Cole-Parmer Stir-pak laboratory mixer) for the flocculation experiments was attached to a metal extension to the flocculation motor. pH was monitored during the initial mixing of the SRW and the flocculation step using a Fisher Scientific Accumet model 10 pH meter. Calibration of the pH meter occurred daily. The temperature of the SRW was recorded once during initial mixing and once during the flocculation step of the experiment using a Cole-Parmer Digi-Sense Thermometer.

Particle aggregation and breakup in the flocculation step was monitored using the Rank Brothers PDA 2000. A full description of the operation of the PDA 2000 is available in the Rank Brothers' PDA 2000 Operating Manual. A simple description is

provided here. Changes in the number of particles present in the SRW causes fluctuations in the light intensity measurements that are recorded by the photodiode of the PDA (Rank Brothers). The PDA then converts light intensity measurements into a two-component (AC-DC) voltage, and following a Poisson distribution, Root Mean Square (RMS) values are developed for the fluctuations in the amplified AC component of the voltage (Rank Brothers). RMS values have previously been used to identify the state of aggregation in a flowing suspension (Gregory and Nelson, 1984). The trend is that the larger the RMS value, the greater the state of aggregation of the flowing suspension. Ratio values were reported digitally by the PDA by converting the RMS values using the following equation:

$$Ratio = \frac{RMS}{DC} \times 10 \tag{6}$$

Ratio values are proportional to RMS values signifying that Equation 6 indicates the state of aggregation in a flowing suspension also.

A peristaltic pump (Cole-Parmer's Masterflex L/S Economy Drive Easy-Load II Pump) with plastic tubing (diameter of 3.0 mm) extracted a constant sample of the SRW during the flocculation step of the experiments. The pump was located downstream from the PDA. The tubing size was selected because of the dilute, low turbidity suspension of the SRW (Rank Brothers). Insufficient transmitted light may occur when using less than 3 mm tubing on concentrated suspensions (Rank Brothers). In addition, smaller tubing size may result in excessive shear by flow and cause breakup of flocculated particles (Gregory, 1981). The flow to the PDA was recirculated back to the flocculation reactor. The Ratio values obtained from the PDA

were recorded using National Instruments NI-DAQ Data Acquisition Driver Software and later imported into Microsoft Excel spreadsheets for analysis.

Experimental procedure

Components of the SRW were mixed together in the flocculation reactor using the rapid mixer at approximately 500 rpm for 30 minutes. During this time period pH adjustments were provided, and the temperature of the water was monitored. Flocculation experiments were conducted at room temperature (22 ± 1 °C). Additionally, the rate of flow through the PDA tubing was adjusted to approximately 19 mL/min to ensure minimal shearing of the flocs during the flocculation step of the experiment (Rank Brothers).

Following the blending of the SRW, the rapid mixer was increased to approximately 600 rpm and the coagulant dose was added. The coagulant/SRW mixture was allowed to mix thoroughly for 1 minute. 50 seconds into the rapid mix process, the data recorder was started to ensure capturing Ratio values at the very beginning of the flocculation process.

At the end of the one-minute rapid mix step, the rapid mixer was shut off and removed from the reactor. The flocculation mixer was then started at the appropriate *G* value. The mixture was flocculated for approximately 29 minutes. The pH and temperature were checked during the flocculation process. In addition, Ratio values and time measurements are recorded.

Analysis of PDA data

Graphical representation of the data was provided by Ratio curves displaying the time dependent collection of Ratio values during the flocculation step. The two types of Ratio curves obtained from the experiments are shown in Figure 2. In Figure 2, the initial growth region describes the stage where floc growth rate exceeds the breakup rate of the floc. The growth is noted as the linear portion of the region. One or two steady-state regions may exist following the initial growth region. Steady-state regions describe a balance between floc growth and breakage where the floc size distribution no longer changes with time (Reich and Vold, 1959; Parker *et al.*, 1972; Lu and Spielman, 1985; Oles, 1992; Spicer, 1995). Figure 2a is a typical Ratio curve with one steady-state region, whereas Figure 2b displays a typical Ratio curve with two steady-state regions. In this study, a second steady-state region was noted at higher G values ($G \geq 70$ s^{-1} and occasionally at $G = 50$ s^{-1}). Research has shown that a more homogeneous, less porous floc has been observed following the breakup and reflocculation of flocs (Clark and Flora, 1991). Here reflocculation was not a step in the experimental procedure. However, it is thought that the reduction in Ratio value and variance of the Ratio value moving from the first to the second steady-state region is the result of the erosion of primary particles from the floc structure due to prolonged shearing. In addition, this second steady-state region may be associated with the development of a more homogeneous and dense floc structure (Figure 3). Research has indicated that prolonged shearing and mixing at intermediate shear rates (i.e., G = 64 to 80 s^{-1}) has led to floc breakup and restructuring (Selomulya *et al.*, 2000). Rupturing flocs at selected weak points developed strong, dense floc structures with

less porosity (Tambo and Watanabe, 1979a; Oles, 1992). Furthermore, restructuring the floc to a more compact size due to more frequent shearing reduced the steady-state floc size, after reaching a maximum size (Spicer *et al.*, 1996; Selomulya *et al.*, 2000).

Three pertinent calculations were performed to analyze the data collected during the flocculation experiments. These calculations included the slope of the initial growth region, a time-weighted average steady-state Ratio value, and a time-weighted variance of the steady-state Ratio values. The slope of the linear initial growth region indicated the rate at which flocs developed. Similar methods have been used by researchers to analyze aggregation rates (Ching *et al.*, 1994). A best-fit line was constructed for the approximate linear growth region of the Ratio curve (Figure 4). From the best-fit line, the slope was determined as:

$$Slope = \frac{\Delta Ratio}{\Delta Time} \tag{7}$$

The time-weighted average steady-state Ratio value was computed as:

$$\overline{Ratio} = \frac{\sum_{i=1}^{N} (Ratio_i \cdot Time_i)}{\sum_{i=1}^{N} Time_i} \tag{8}$$

$\overline{Ratio}$ represents the state of aggregation obtained over a steady-state time interval.

Obtaining the time-weighted variance of the Ratio values of a steady-state region provided an indicator of the severity of breakup as well as a measure of floc structural differences. Generally, a smaller variance signified a tighter floc size distribution and a more homogeneous, dense, and less porous floc structure in the

sampled reactor region. This concept is explained more thoroughly in a later section. Equation 9 below was used to calculate the time-weighted variance.

$$Variance = \frac{\sum_{i=1}^{N}\left[\left(Ratio_i - AverageRatio\right)^2 \cdot Time_i\right]}{\sum_{i=1}^{N} Time_i} \quad (9)$$

RESULTS AND DISCUSSION

In this study, a constant sweep floc mechanism was selected for the experiments investigating the impact of particle concentration while a fixed particle concentration of 50 mg/L was used to study the impact of coagulation mechanism. As discussed earlier, a second steady-state region in the Ratio value was found with higher G values (≥ 70 s^{-1} and occasionally at 50 s^{-1}). The second region represented the final state of aggregation in the higher G experiments. The Ratio values along with the variance in these regions were used to develop Figures 5 – 7.

In this study, significant overloading occurred at $G = 40$ s^{-1} for the 100 mg/L concentration. The PDA gain controls were used to amplify the AC and DC signals to provide meaningful Ratio values to the flocs in the flowing suspension (Rank Brothers). Gain controls were left constant over all experimental conditions to compare the results between the three different experimental conditions. However, considering the large range of possible floc sizes, significantly large flocs could provide a voltage that is larger than the peak voltage of the amplified AC signal overloading the PDA (Rank Brothers).

Producing flocs larger than what is measurable by the PDA under the existing gain control settings provides Ratio values that are less than what actually pertain to the floc sizes in the flowing suspension (Rank Brothers). Substantial overload to the PDA, as experienced with the larger SRW particle concentration at $G = 40\ s^{-1}$, skewed the Ratio values recorded. This directly provided erroneous results for the analysis of the initial growth rate, steady-state Ratio value, and steady-state variance. Therefore, data collected under these experimental conditions has been left out for discussion (note Figures 5 – 7). It is thought that if proper gain control settings were available for the range of floc sizes encountered, the data would conform to trends observed for the lower particle concentration.

Impact of SRW particle concentration and coagulation mechanism on floc growth

Figure 5 displays the floc growth determined at different reactor regions for the two particle concentrations and coagulation mechanisms over the range of G values tested. Slope values of the linear growth region were averaged for several experiments. In Figure 5, floc growth was found to increase with increasing G regardless of particle concentration or coagulation mechanism. As seen by others, the higher growth rates are the result of more particle collisions occurring with increased G (Ching *et al.*, 1994; Selomulya *et al.*, 2000). As shown in Figure 5, increasing the number of particles in suspension also increased floc growth. A greater particle concentration in the SRW increased the particle collision frequency throughout the reactor. These results are consistent with the findings of Burns *et al.* (1997) in their

investigation of the impact of particle concentration on a colloid system with a low salt level (< 1 M KNO_3) concentration.

The results in Figure 5 also showed that floc growth was larger in the bulk region than in the impeller discharge region at lower G values (i.e. G = 40 s^{-1} to occasionally 50 s^{-1}). Cluster-cluster collisions have been used to characterize aggregation in the bulk region (Ducoste, 2002). As discussed in Ducoste (2002), at low G, the bulk region may contain chaotic and non-chaotic zones. Research has shown that floc collision is favored at the boundaries of these chaotic and non-chaotic zones in the bulk region (Danielson *et al.*, 1991; Hansen and Ottino, 1996). As a result, cluster-cluster aggregation would be favored in the bulk region making the growth rate seem larger. In the impeller region, particle collision is mostly dominated by primary-primary or primary-cluster aggregation. The resulting growth rate in the impeller discharge region would consequently be lower due to these types of particle collisions. These collision patterns are the result of the turbulence heterogeneity and may be the result of the magnitude of aggregation time scales versus the reactor circulation time scales.

As the shear rate increases, flocs enter the viscous shearing impeller region more frequently (Griffiths, 1996). As G increased, floc growth at both reactor locations collapsed to the same value (Figure 5). However, the convergence of these two growth rates was found to depend on both the initial particle concentration and the coagulation mechanism. For the 50 mg/L particle concentration, the bulk and impeller region growth rate converged beyond G = 70 s^{-1}. The 100 mg/L particle concentration data showed that floc growth had not reached convergence up through the largest G

tested (G = 90 s^{-1}). As discussed earlier, cluster-cluster collisions may be more pronounced at higher particle concentrations in the bulk region at the border of these chaotic and non-chaotic regions. This action would further push the time scales of collisions towards the reactor circulation time scales and, hence, increase the *G* required to produce growth rate convergence between the impeller discharge region and bulk region.

In Figure 5, the results showed higher floc growth moving from the charge neutralization mechanism to the sweep floc mechanism. In sweep floc, the precipitate, $Al(OH)_3(s)$, a product of hydrolyzing alum, develops an amorphous floc structure with porous openings available to enmesh suspended particles as it "sweeps" through the suspension (Reynolds and Richards, 1996). Charge neutralization involves reducing the diffusive layer of suspended particles by lowering the energy required for other suspended particles to contact one another through adsorption of the coagulant onto suspended particle surfaces (Letterman *et al.*, 1999). It was found that greater particle collision efficiency occurred between less dense, porous flocs, as seen with the sweep floc mechanism, compared to that observed with solid particles (Kusters *et al.*, 1997). Increasing collision efficiency will increase the floc growth rate and produce larger sizes.

Charge neutralization data, unlike that of the sweep floc data, supplied similar floc growth for both reactor regions over the entire range of *G* values tested (Figure 5). These results suggest that particle collisions were not enhanced at the boundaries of chaotic and non-chaotic zones in the bulk region at low *G*. Moreover, flocs formed under charge neutralization may have aggregation time scales that were considerably

larger than the circulation time scales of the reactor. As a result, floc growth in the reactor never exhibited a heterogeneous quality at lower *G* values.

Impact of SRW particle concentration and coagulation mechanism on steady-state Ratio value

Figure 6 displays the impact of particle concentration and coagulation mechanism on the Ratio values determined at different reactor locations as a function of *G*. In Fig. 6, the results showed that the Ratio values decreased as *G* increased regardless of particle concentration and coagulation mechanism. As confirmed by others, higher breakup rates were shown to decrease floc size as *G* increased (Oles, 1992; Parker *et al.*, 1972; Tambo and Watanabe, 1979a; Spicer and Pratsinis, 1996; Selomulya *et al.*, 2000). The range of flocs vulnerable to breakup increases as flocs grow (Kusters, 1991). Considering floc growth proved to increase at higher shear rates (Selomulya *et al.*, 2000; Ching *et al.*, 1994), larger *G* values would also increase the breakup rate and the range of flocs affected. The end result is a flocculation environment that produces a smaller steady-state mean floc size in a shorter amount of time with increasing *G* values.

In Figure 6, increasing the particle concentration of the SRW increased the Ratio value over the range of *G* values tested. Particle collisions are more frequent with a larger number of particles present in the reactor and, as a result, produce a larger floc size. Researchers have suggested that cluster-cluster collisions of the bulk region flocs (Ducoste, 2002) with a looser and weaker floc structure (Oles, 1992; Tang *et al.*, 2001) formed larger flocs at lower *G* values. These larger, weaker flocs would then be fractured as a result of the larger scales of turbulent fluctuating velocities in

the impeller discharge region (Ducoste, 2002). The results in Figure 6 seems to slightly confirm that possible scenario since the Ratio value of the bulk region was greater than the impeller discharge region Ratio value at $G < 70\ s^{-1}$.

As G increased, the Ratio values obtained in the two different reactor regions merged to the same value for both tested particle concentrations (Figure 6). Data collected for both the 50 mg/L and 100 mg/L concentration indicated that near $G = 70\ s^{-1}$, little difference was found in the floc size between the impeller discharge region and the bulk region. At higher G values, the flocs are circulated more frequently through to the impeller discharge region where any loosely attached particles to a floc created in the bulk region are eroded. The remaining floc has a stronger floc binding energy similar to the flocs formed from primary-primary collisions (Yeung *et al.*, 1997; Dyer and Manning, 1999).

In Figure 6, the results clearly showed that sweep floc coagulation produced larger Ratio values than charge neutralization coagulation over the range of G values tested. This trend supports the difference noted earlier in floc structure between the two different coagulation mechanisms. The results suggest that tighter, less porous floc structures are developed using the charge neutralization mechanism, whereas the amorphous floc structure of sweep floc provides a less dense, porous, and larger floc.

At lower G values, there still existed a slight variation in the Ratio values obtained between the different reactor locations for both coagulation mechanisms tested (Figure 6). Larger flocs were still found in the reactor's bulk region using the sweep floc mechanism at the lower G values. With large circulation time scales, the amorphous sweep floc structure in the bulk region was less disturbed by the higher

shearing of the impeller discharge region. However, as the *G* increased, circulation time decreased, and the large bulk region flocs more frequently encountered the higher viscous shearing region (Griffiths, 1996). The looser floc structures of the bulk region (Oles, 1992; Tang *et al.*, 2001) ruptured into smaller flocs. These smaller flocs are stronger than the original bulk flocs from which they were derived due to greater primary-primary collisions (Yeung *et al.*, 1997; Dyer and Manning, 1999). The breakup of the bulk region flocs generated a floc size similar to those of the impeller discharge region producing a homogeneous floc environment in the reactor.

However, at lower *G*, larger Ratio values were determined for the impeller discharge region using charge neutralization (Figure 6). Recall that reducing the diffusive layer around suspended particles lessens the amount of energy required to move particles into contact with one another (Letterman *et al.*, 1999). The impeller discharge region had considerably more energy to offer particle collisions than the bulk region. Moreover, the floc structure formed with charge neutralization is more similar to flocs developed from primary-primary collisions than those created from cluster-cluster collisions. This indicates that with charge neutralization, primary-primary collisions, not cluster-cluster collisions, drive the collision frequency rates. Since most primary-primary collisions occur in the impeller discharge region at a higher rate, a larger mean floc size is expected in this region. With a higher *G*, the circulation time of the reactor is considerably shorter than the time scales of aggregation. Circulating the bulk region flocs into the impeller discharge region more frequently ensured greater primary-primary collisions. Flocs from both reactor regions

experienced similar collision frequencies that resulted in a common Ratio value at higher *G*.

Impact of SRW particle concentration and coagulation mechanism on steady-state variance

Figure 7 displays the variance values determined at different reactor regions for the different particle concentrations and coagulation mechanisms over the range of *G* values tested. In Figure 7, the results showed that variance decreased as *G* increased within the reactor. A large variance value indicates that a wider range of floc sizes exists at that specific location. A wider range of floc sizes at the lower *G* values (i.e. greater variance) may suggest that larger particles were being formed in the bulk region than in the impeller discharge region. These larger bulk region flocs are then broken up in the impeller discharge region.

As mentioned in the materials and methods section, a second steady-state region was produced at $G \geq 70$ s^{-1} and occasionally at $G = 50$ s^{-1} (Figure 2b). Spicer and Pratsinis (1996) found that at low alum concentrations (4.3 and 10.7 mg/L), the geometric standard deviation, which is the square root of the variance, of a steady-state floc size distribution decreased as shear rate increased. Spicer and Pratsinis (1996) showed that the decrease in the standard deviation is due to trimming the large tail of the floc size distribution while the small tail remained unchanged approximating the size of the primary particles. Interestingly, the second steady-state region was found to produce a smaller variance than the first steady-state region. It is thought that a similar phenomenon occurs as that seen by Spicer and Pratsinis (1996). For experiments exhibiting two steady-state regions, the restructuring of larger flocs in

the bulk region may occur from the erosion of primary particles from the structure due to prolonged exposure to high shear stresses, thus trimming the large tail of the floc size distribution. The smaller flocs are relatively unaffected by the higher shear stresses, so that the range of the floc size distribution is reduced mainly due to large floc erosion and restructuring. Therefore, the variance in this study could be considered an indicator of floc structure changes. However, further investigation is required to determine whether variance could measure floc structure changes at low *G* values considering little breakup occurs at the lower shear stresses.

In this study, increasing the particle concentration was found to increase the variance in the Ratio values (Figure 7). The increased number of particles available for collision encouraged the formation of a larger, more heterogeneous range of floc sizes. As discussed earlier, a large variance indicates the formation of flocs that are porous, relatively weak, and have a low *D* value. Past experimental research has proven that as more primary particles were added to growing flocs with a *D* less than the Euclidean dimension, floc density decreased coupled with an increase in porosity (Clark and Flora, 1991). Therefore, variance may also describe the floc structure observed due to changes in particle concentration. Considering this interpretation of variance, a larger variance found for the higher particle concentration seems to further confirm the findings of Clark and Flora (1991).

The results in Figure 7 clearly show that at low *G* values the variance in the bulk region is lower than that in the impeller discharge region confirming that a majority of the breakup occurs in the impeller discharge zone. This was true regardless of particle concentration. At lower *G* values the shear rates generated in the impeller

discharge region will cause the fracture of bulk region flocs into particles much larger than the primary particle size as well as the erosion of primary particles from these larger flocs. The result is a wide distribution of particle sizes in that zone. In the bulk region, breakup occurs at a much lower rate. As a result, the particle distribution should be narrower (i.e. smaller variance). This means that flocs in the bulk region may be allowed to form larger aggregates due to the preferential concentration of particles at chaotic/non-chaotic boundaries without being fractured until they recirculate into the impeller discharge zone.

As G increased, the variance tends to decrease due to a higher breakup rate from the higher shear stresses in the reactor (Figure 7). In addition, Figure 7 clearly shows that the variance in the bulk and impeller discharge region tends to merge as G increases. Convergence of the bulk and impeller discharge region variance occurred at a higher G value with increasing particle concentration (G = 70 s^{-1} for the 50 mg/L concentration; G = 90 s^{-1} for the 100 mg/L concentration). As discussed earlier, the higher particle concentration tends to further increase the collision rate in the bulk region at the locations where particles are preferentially concentrated (i.e. chaotic/non-chaotic boundaries). Therefore, a higher circulation frequency and impeller discharge region breakup rate is needed to force a homogeneous floc size distribution in the reactor.

Performance of the experiments with different coagulation mechanisms revealed that charge neutralization created less variance in the distribution of flocs in the reactor (Figure 7) than with sweep floc. As mentioned earlier, charge neutralization creates a much tighter, condensed floc structure leaving less chance for

variation in floc size as a result of breakup. Flocs formed under sweep floc tend to have open floc structures that are better designed to "sweep" out suspended particles essentially offering several possible locations on the floc surface for particles to attach. However, this open structure produces weaker flocs whose large particles could be easily fractured and generate a wider distribution of particle sizes.

Under charge neutralization, greater variance in floc size was still found in the impeller discharge region at lower G values although the difference between that region and the bulk region was much less than that under sweep floc conditions (Figure 7). Charge neutralization data indicated a homogeneous variance at $G = 55\ s^{-1}$, which is less than that found with sweep floc ($G = 70\ s^{-1}$). These results suggest that the coagulation mechanism plays a significant role in altering the collision rates in both the impeller discharge and bulk region.

CONCLUSIONS

Experimental research was conducted to determine the impact of heterogeneous turbulence on the flocculation performance of a bench-scale reactor. The impact of the G value, particle concentration, and coagulation mechanism on the aggregation and breakup processes were also investigated. The floc growth rate, steady-state mean size and variance of the steady-state floc sizes were developed from PDA Ratio values over the course of the flocculation experiment. These calculations were determined for the two sampled regions of the reactor. Performance and analysis of the flocculation experiments yielded these findings:

- Floc growth increased as *G* increased, regardless of particle concentration or coagulation mechanism, as greater particle collision frequency accompanied greater shearing rates. Greater particle concentration increased particle collision frequency in the reactor generating greater floc growth. Moreover, greater floc growth was achieved with flocs produced with sweep floc coagulation mechanism than with the charge neutralization mechanism.
- The flocculation results confirmed previous research that the mean floc size dropped as *G* increased, regardless of the particle concentration or coagulation mechanism. Furthermore, increasing the number of particles in the SRW increased the floc size developed in the reactor. In addition, larger flocs were also generated by the amorphous, less dense sweep floc structures than by the tighter flocs formed with charge neutralization.
- The variance in the floc size distribution decreased as *G* increased within the reactor, regardless of particle concentration and coagulation mechanism. The results showed a larger variance with an increase in particle concentration. The increased number of particles in the SRW encouraged the formation of a greater range of floc sizes from primary-primary, primary-cluster, and cluster-cluster collisions. Steady-state floc size variation was less when using the charge neutralization mechanism due to the tight, condensed floc structures developed.
- Differences in floc growth, size, and variance in the steady-state floc sizes in different reactor regions were also found to depend upon the *G* value, particle concentration, and coagulation mechanism. It is thought that preferential concentration developed along boundaries of chaotic/non-chaotic regions along

with differences between aggregation and circulation time scales were the main reason for these differences. All but the charge neutralization floc growth data point towards a heterogeneous environment at low *G* values, with a shift towards a homogeneous environment at high *G* values. Additionally, variance was found to provide a measure of relative changes in floc structure with changes in *G* values, particle concentration, and coagulation mechanism, although further investigation is required to determine whether variance is a realistic parameter to judge structural changes in flocs at low *G* values.

The results seem to indicate how turbulent heterogeneity has a noticeable impact on flocculation performance at low G values. The information from this study could be important for future population balance model (PBM) development for modeling flocculation performance in a heterogeneous turbulent environment. In addition, the impact of factors such as water quality, temperature, and coagulation dose on flocculation performance at low G values has not been thoroughly examined. Experiments analyzing the impact of such factors would be necessary to develop a more comprehensive model that considers most influential factors on the flocculation performance in a drinking water treatment plant.

REFERENCES

Argaman, Y. and Kaufman, W.J. (1970) Turbulence and flocculation. Journal of Sanitary Engineering Division ASCE, **SA2**, 223.

Bremer, L.G.B., Walstra, P., and van Vliet, T. (1995) Estimations of the aggregation time of various colloidal systems. Colloids and Surfaces A: Physiochemical and Engineering Aspects **99** (2), 121-127.

Burns, J.L., Yan, Y.D., Jameson, G.J., and Biggs, S. (1997) A light scattering study of the fractal aggregation behavior of a model colloidal system. Langmuir **13** (24), 6413-6420.

Camp, T.R. and Stein, P.C. (1943) Velocity gradients and internal work in fluid motion. Journal of the Society of Civil Engineering **30**, 219-237.

Ching, H.W., Tanaka, T.S., and Elimelech, M. (1994) Dynamics of coagulation of kaolin particles with ferric chloride. Water Research **28** (3), 559-569.

Clark, M.M, Srivastava, R.M., Lang, J.S., Trussell, R.R., McCollum, L.J., Bailey, D., Christie, J.D., and Stolarik, G. (1994) Selection and design of mixing processes for coagulation. AWWARF Report, Denver, CO.

Clark, M.M. and Fiessinger, F. (1991) Mixing and scaleup in mixing in coagulation and flocculation. AWWARF, Denver, CO.

Clark, M.M. and Flora, J.R.V. (1991) Floc restructuring in varied turbulent mixing. Journal of Colloid and Interface Science **147** (2), 407-421.

Danielson, T.J., Muzzio, F.J., and Ottino, J.M. (1991) Aggregation and structure formation in chaotic and regular flows. Physical Review Letters **66** (24), 3128-3131.

Drobny, N.L. (1963) Effect of paddle design in flocculation. Journal of Sanitary Engineering Division, ASCE **SA2**, 17.

Ducoste, J.J. (2002) A two-scale PBM for modeling turbulent flocculation in water treatment processes. Chemical Engineering Science, in press.

Ducoste, J.J. and Clark, M.M. (1998) The influence of tank size and impeller geometry on turbulent flocculation I: Experimental. Environmental Engineering Science **15** (3), 215-224.

Ducoste, J.J., Clark, M.M., and Weetman, R.J. (1997) Turbulence in flocculators: The effects of tank size and impeller type. AICHE **43** (2), 328-338.

Dyer, K.R. and Manning, A.J. (1999) Observation of the size, settling velocity, and effective density of flocs and their fractal dimensions. Journal of Sea Research **41** (1-2), 87-95.

Eaton, J.K. and Fessler, J.R. (1994) Preferential concentration of particles by turbulence. International Journal of Multiphase Flow **20** (Supp.), 169-209.

Francois, R.J. (1987) Strength of aluminum hydroxide flocs. Water Resources **21** (9), 1023-1030.

Greenberg, A.E., Clesceri, L.S., and Eaton, A.D. (1992) Standard methods for the examination of water and wastewater. APHA, AWWA, and WEF, Washington, D.C., 2-25-2-28.

Gregory, J. (1981) Flocculation in laminar tube flow. Chemical Engineering Science **36**, 1789-1794.

Gregory, J. and Nelson, D.W. (1984) In solid-liquid separation. Ellis Horwood, Chichester, 172-182.

Griffiths, S. (1996) Journal of CIWEM **10**, 324.

Han, M. and Lawler, D.F. (1991) Interaction of two settling spheres; Settling rates and collision efficiencies. Journal of Hydraulics Division, ASCE **17** (10), 56-73.

Hansen, S. and Ottino, J.M. (1996) Aggregation and cluster size evolution in nonhomogeneous flow. Journal of Colloid and Interface Science **179** (1), 89-103.

Hanson, A.T. and Cleasby, J.L (1990) Effect of temperature on turbulent flocculation: Fluid dynamics and chemistry. Journal AWWA **82** (11), 56-73.

Hsu, J.P. and Glasgow, J.B. (1983) Floc size reduction in the turbulent environment. Particulate Science and Technology **1**, 205.

Jiang, Q. and Logan, B.E. (1996) Fractal dimensions of aggregates from shear devices. Journal AWWA **88** (2), 100.

Kramer, T.A. and Clark, M.M. (2000) Modeling orthokinetic coagulation in spatially varying laminar flow. Journal of Colloid and Interface Science **227** (2), 251-261.

Kusters, K.A. (1991) The influence of turbulence on aggregation of small particles in agitated vessels. Ph.D. thesis, Eindhoven University of Technology, The Netherlands.

Kusters, K.A., Wijers, J.G., and Thoenes, D. (1997) Aggregation kinetics of small particles in agitated vessels. Chemical Engineering Science **52** (6), 107-121.

Letterman, R.D., Amirtharajah, A., and O'Melia, C.R. (1999) Water quality and treatment: A handbook of community water supplies. McGraw-Hill, New York, 6.47-6.48.

Lu, C.F. and Spielman, L.A. (1985) Kinetics of floc breakage and aggregation in agitated liquid suspensions. Journal of Colloid and Interface Science **103**, 95-105.

Maxey, M.R. (1987) The gravitational settling of aerosol particles in homogeneous turbulence and random flow fields. Journal of Fluid Mechanics. **174**, 441-465.

McConnachie, G.L. (1991) Turbulence intensity of mixing in relation to flocculation. Journal of Environmental Engineering **117** (6), 731-750.

Oldshue, J.Y. and Mady, O.B. (1978) Flocculation performance of mixing impellers. Chemical Engineering Progress **74** (8), 103-108.

Oldshue, J.Y. (1983) Fluid Mixing Technology. McGraw-Hill, New York, 306.

Oles V. (1992) Shear-induced aggregation and breakup of polystyrene latex particles. Journal of Colloid and Interface Science **154** (2), 351-358.

Parker, D.S., Kaufman, W.J., and Jenkins, D. (1972) Floc breakup in turbulent flocculation processes. Journal of Sanitary Engineering Division, ASCE **SA1**, 79-99.

Patwardhan, S.V. and Mirajgaonkar, A.J. (1970) Hydraulics of flocculation and paddle characteristics. Journal of the Institute of Engineering (India) Public Health **50**, 60.

Photometric dispersion analyzer PDA 2000 operating manual. Rank brothers LTD. Cambridge, England.

Reade, W.C. and Collins, L.R. (2000) Effect of preferential concentration on turbulent collision rates. Physics of Fluids **12** (10), 2530-2540.

Reynolds, T.D. and Richards, P.A. (1996) Unit operations and processes in environmental engineering. PWS Publishing Company, Boston, 173.

Reich, I. and Vold, R.D. (1959) Flocculation-deflocculation in agitated suspensions. I. Carbon and ferric oxide in water. Journal of Physical Chemistry **63**, 1497-1501.

Saffman, P.G. and Turner J.S. (1956) On the collision of drops in turbulent clouds. Journal of Fluid Mechanics **1**, 16-30.

Sajjad, M.W. and Cleasby, J.L. (1995) Effect of impeller geometry and various mixing pattern on flocculation kinetics of kaolin clay using ferric salt. Proceedings of AWWA National Conference, Anaheim, CA.

Schwartzberg, H.G. and Treybal, R.E. (1968) Fluid and particle motion in turbulent stirred tanks. Ind. Eng. Chem. Fundamentals **7**, 1-12.

Selomulya, C., Amal, R., Bushell, G., and Waite, T.D. (2001) Evidence of shear rate dependence on restructuring and breakup of latex aggregates. Journal of Colloid and Interface Science **236** (1), 67-77.

Sonntag, R.C. and Russel, W.B. (1987) Structure and breakup of flocs subjected fluid stresses II: Theory. Journal of Colloid and Interface Science **115** (2), 378-389.

Spicer, P.T. (1995) The dynamics of shear-induced flocculation in a stirred tank. M.S. thesis, University of Cincinnati, Ohio.

Spicer, P.T. and Pratsinis, S.E. (1996) Shear-induced flocculation: The evolution of floc structure and the shape of the size distribution at steady-state. Water Research **30** (5), 1049-1056.

Spicer, P.T., Keller, W., and Pratsinis, S.E., (1996) The effect of impeller type on floc size and structure during shear-induced flocculation. Journal of Colloid and Interface Science **184** (1), 112-122.

Squires, K.D. and Eaton, J.K. (1991) Preferential concentration of particles by turbulence. Physics of Fluids A **3** (5), 1169-1178.

Tambo, N. and Watanabe, Y. (1979) Physical aspect of flocculation process I. Fundamental treatise. Water Research **13**, 429-439.

Tang, S., Ma, Y., and Shiu, C. (2001) Modeling the mechanical strength of fractal aggregates. Colloids and Surfaces A: Physicochemical and Engineering Aspects **180** (1), 7-16.

Thomas, D.G. (1964) Turbulent disruption of flocs in small particle size suspensions. AICHE **10** (4), 517-523.

Wang, L.P. and Maxey, M.R. (1993) Settling velocity and concentration distribution of heavy particles in homogeneous isotropic turbulence. Journal of Fluid Mechanics **256**, 27-68.

Yeung, A., Gibbs, A., Pelton, R. (1997) Effect of shear on the strength of polymer-induced flocs. Journal of Colloid and Interface Science **196** (1), 113-115.

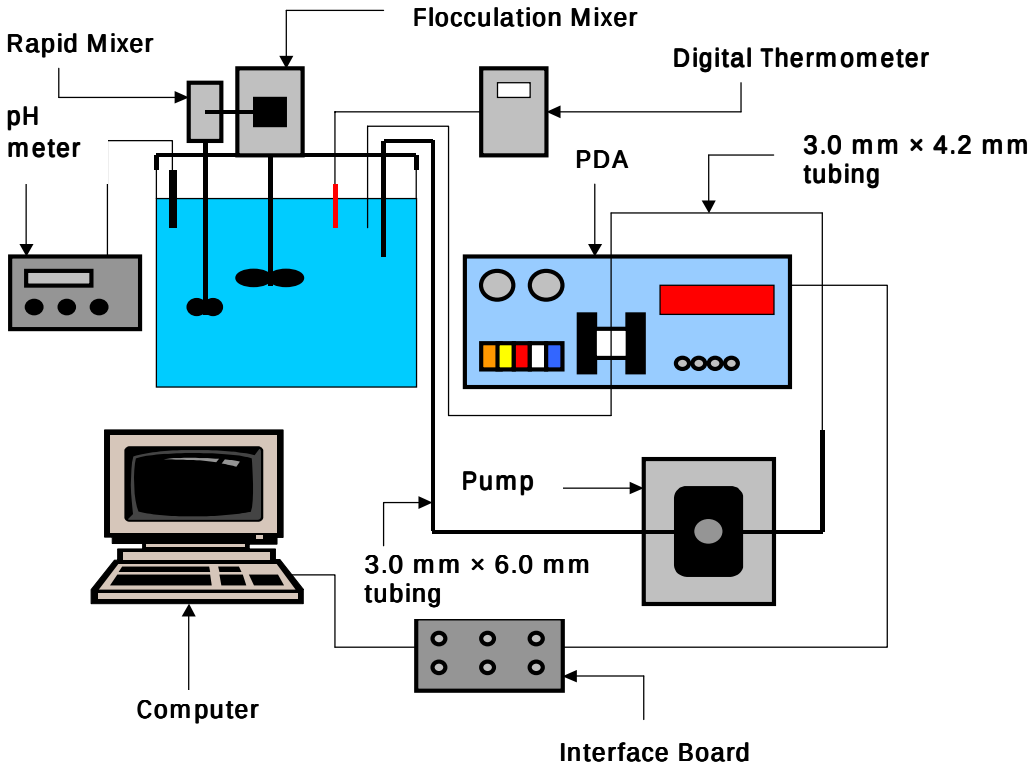

Figure 1. Experimental setup.

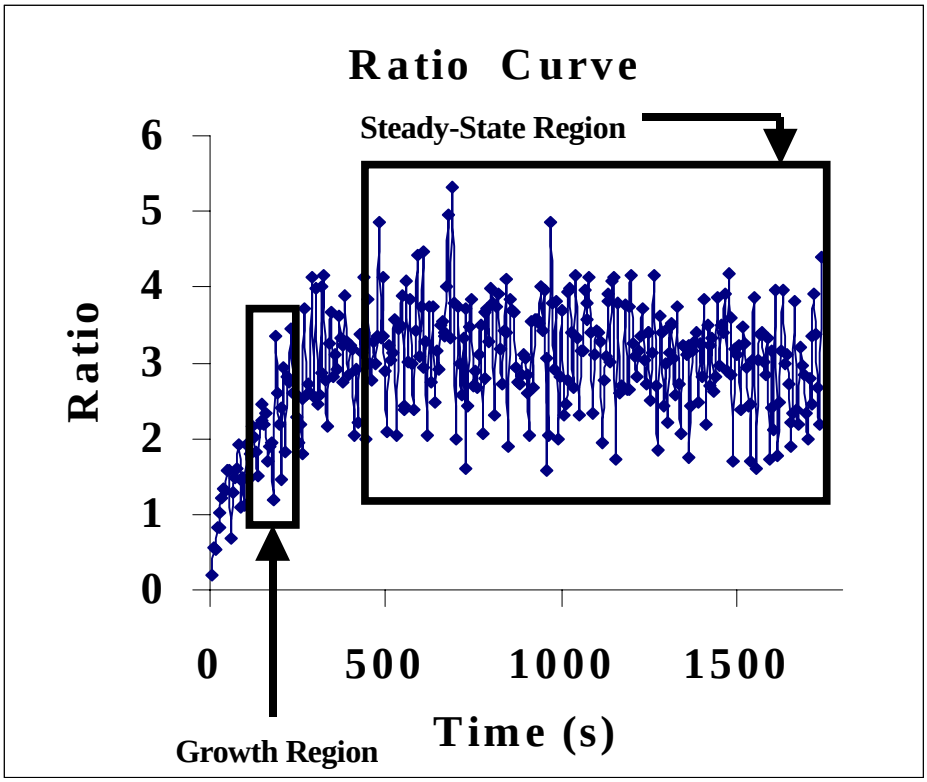

Figure 2a. Ratio curve with one steady-state region.

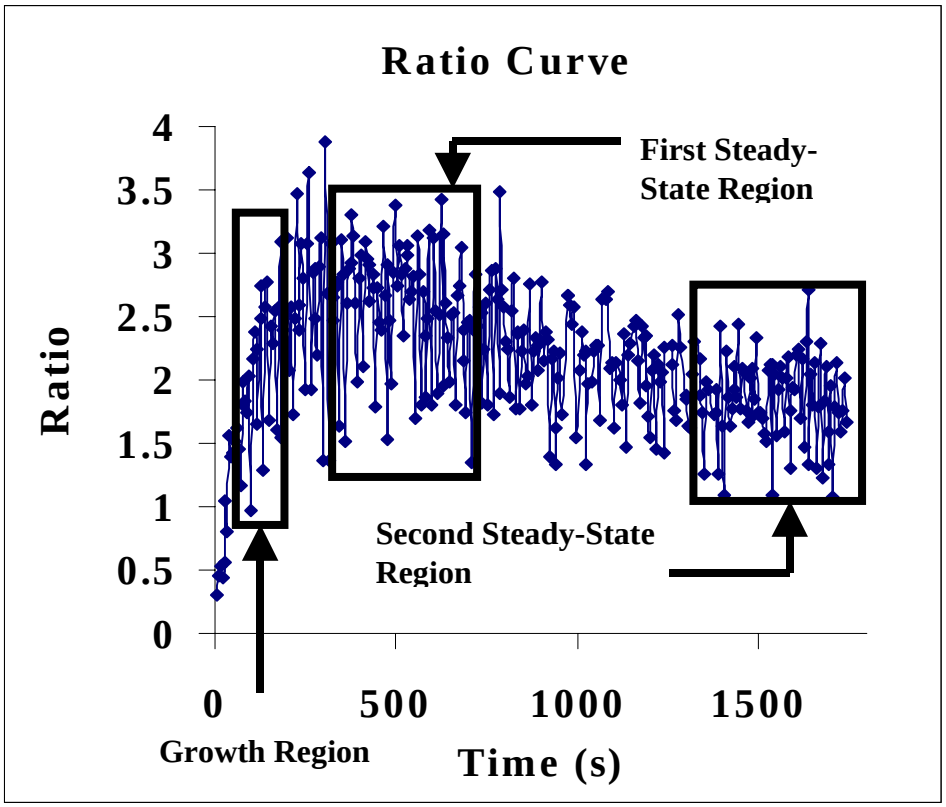

Figure 2b. Ratio curve with two steady-state regions.

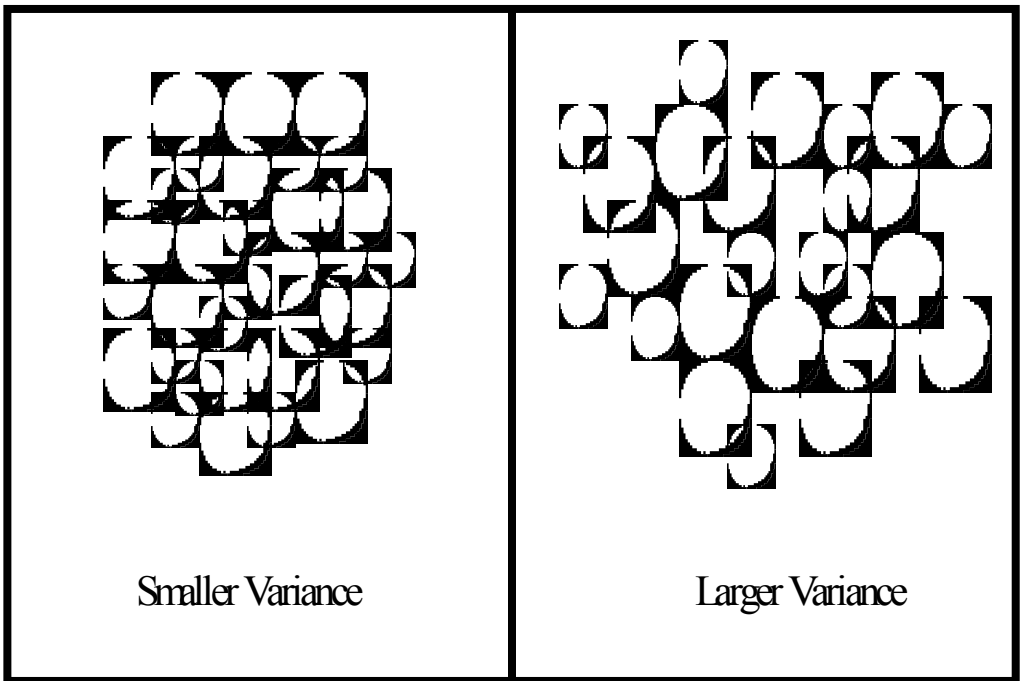

Figure 3. Differences in floc structure and its association to variance.

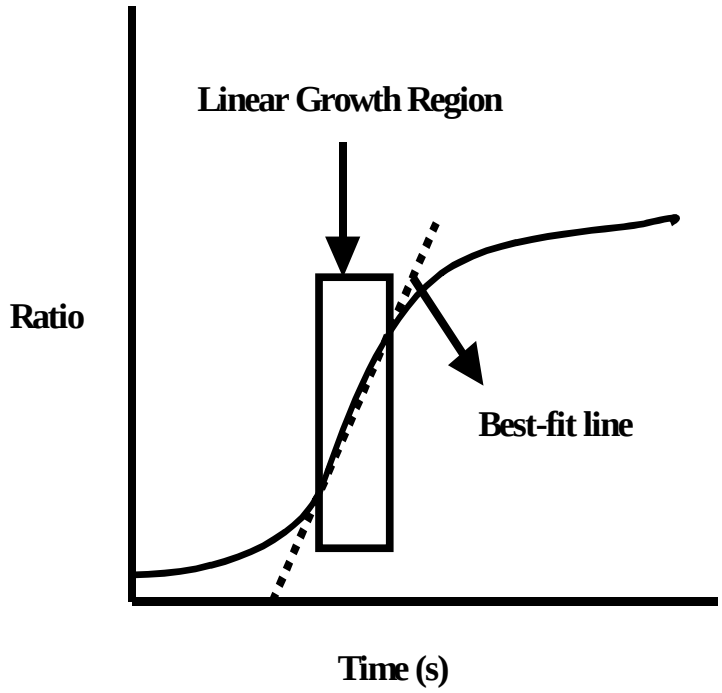

Figure 4. Best-fit line approximation of linear growth region.

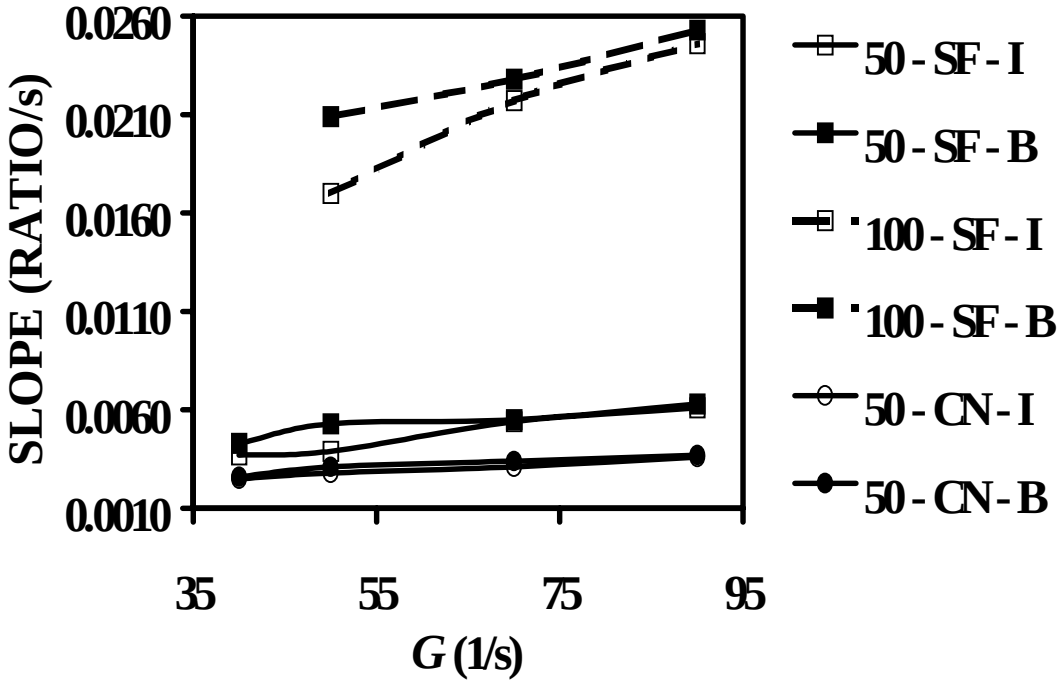

Figure 5. Slope vs. *G* value.
Comparison of floc growth at different experimental conditions. 50 = 50 mg/L; 100 = 100 mg/L; SF = sweep floc; CN = charge neutralization; I = impeller discharge region; B = bulk region.

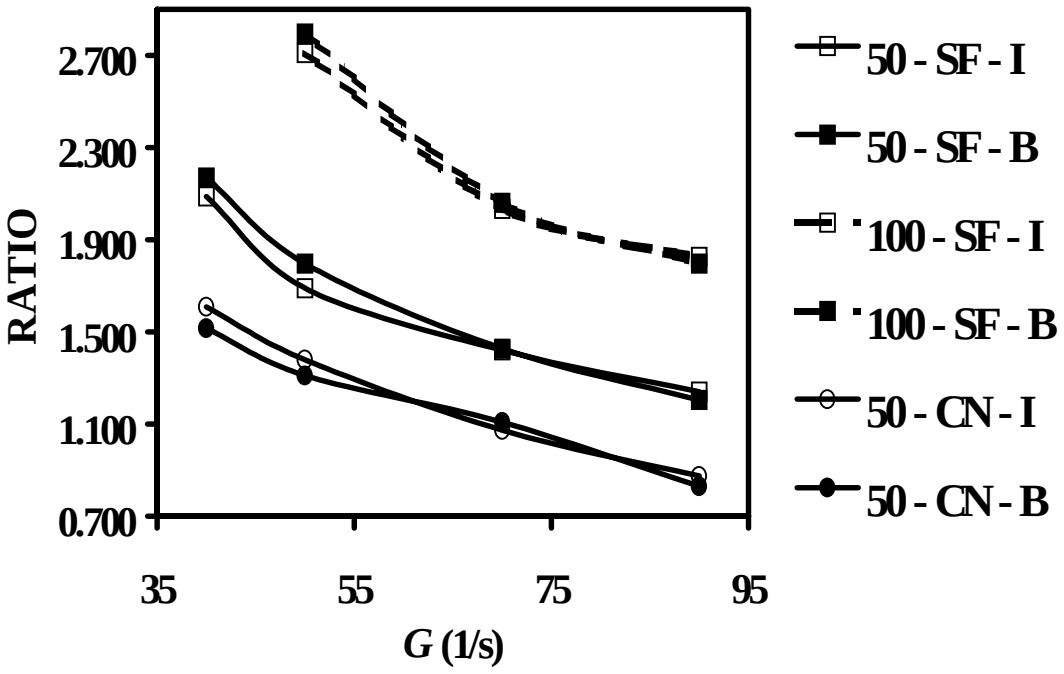

Figure 6. Ratio vs. *G* value.
Comparison of floc size at different experimental conditions. 50 = 50 mg/L; 100 = 100 mg/L; SF = sweep floc; CN = charge neutralization; I = impeller discharge region; B = bulk region.

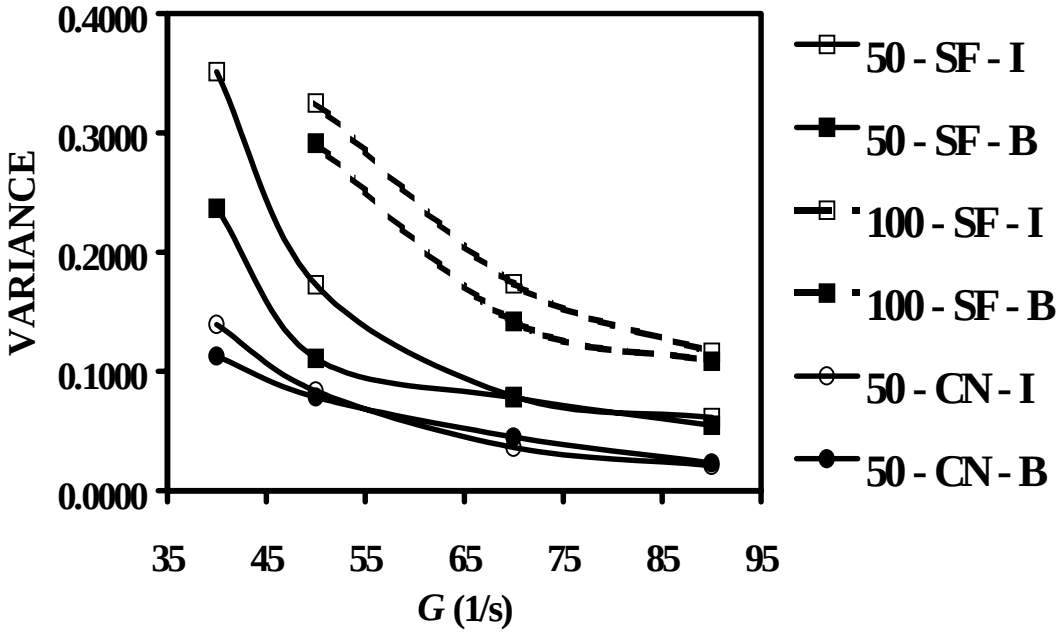

Figure 7. Variance vs. *G* value.
Comparison of the variance in the steady-state floc sizes at different experimental conditions. 50 = 50 mg/L; 100 = 100 mg/L; SF = sweep floc; CN = charge neutralization; I = impeller discharge region; B = bulk region.

Table 1. Experimental conditions.

Test Condition #	Kaolin Clay Particle Concentration (mg/L)	Coagulation Mechanism	pH	Alkalinity (mg/L $CaCO_3$)
1	50	Sweep Floc	8.0	83.0
2	100	Sweep Floc	8.0	83.0
3	50	Charge Neutralization	6.0	160.0

Table 2. Experimental SRW component additions.

Test Condition (Coagulation Mechanism – Particle Concentration)	Volume DI Water (L)	Mass Kaolin Clay (g)	Normality H_2SO_4 (N)	Volume H_2SO_4 (mL)	Volume 1N Na_2CO_3 (mL)
Sweep Floc – 50 mg/L	28.0	1.4	0.2	98.0	234.0
Sweep Floc – 100 mg/L	28.0	2.8	0.2	49.0	109.0
Charge Neutralization – 50 mg/L	28.0	1.4	0.8	95.0	89.5

Table 3. Alum dosage and volumetric additions.

Test Condition (Coagulation Mechanism – Particle Concentration)	Alum Dosage (mg/L)	Volume 1 g/L Alum (mL)
Sweep Floc – 50 mg/L	9.88	280.0
Sweep Floc – 100 mg/L	9.94	280.0
Charge Neutralization – 50 mg/L	9.33	263.0